

The localization of SP-B and influences of lipopolysaccharide on it

W.-N. WANG^{1,2}, J.-H. ZHOU¹, P. WANG^{2,3}, X.-J. ZHANG²

¹State Key Laboratory of Trauma, Burns and Combined Injury, Department 4, Institute of Surgery Research, Daping Hospital, Third Military Medical University, Chongqing, China

²College of Pharmacy and Bioengineering, Chongqing University of Technology, Bananqu, Chongqing, China

³Center Laboratory, No. 82 Hospital of the Chinese People's Liberation Army, Huaian, China

Abstract. – OBJECTIVE: Surfactant protein B (SP-B) is the only essential protein component of lung surfactant, the relationship between localization and function is very close. The localization of rat SP-B and influences of lipopolysaccharide (LPS) on it were investigated.

MATERIALS AND METHODS: The localization of SP-B protein in lung tissue was detected by immunofluorescence after challenged with intratracheal instillation of LPS. The constructed recombinant plasmid pEGFP-N2-SP-B was transfected with CCI-149 cell lines by liposome to explore the localization of SP-B in alveolar type II epithelial cells. Furthermore, the expression and function of SP-B were analyzed with LPS stimulating.

RESULTS: The proteins SP-B and SP-C showed the same pattern of expression in normal lung, and distributed in the alveolar cavity, LPS can directly affect the expression of SP-B *in vivo*, contrast to SP-B, the LPS-induced influences on SP-C is little. SP-B had the membrane embedded features and localized on the cell surface of CCL149 *in vitro*, but was influenced by LPS.

CONCLUSIONS: It is confirmed that the expression and membrane function of SP-B were decreased by stimulating LPS in lung tissue and alveolar type II epithelial cells.

Key Words:

SP-B, Localization, LPS, Lung, Alveolar type II epithelial cells.

Introduction

Lung surfactant is a complex of lipids and proteins that lines the air-water interface at the alveolar surface. It is essential for reducing surface tension and preventing alveolar collapse, deficiency or inactivation of lung surfactant leads to potentially lethal respiratory disorders. Surfactant

proteins^{1,2} are designated by their chronologic order of discovery as SP-A, SP-B, SP-C, and SP-D³. SP-A and SP-D are water soluble and important for host defense, whereas SP-B and SP-C are smaller hydrophobic proteins that are critical for reducing surface tension during breathing⁴.

SP-B is the only essential protein component of lung surfactant, as evidenced by the lethality of hereditary SP-B deficiency in humans and the lethal effect of knocking out the SP-B gene in mice. SP-B produced by alveolar to lower the surface tension by inserting lipids into the air/liquid interface of the lung is unambiguously necessary for pulmonary function⁵.

Inflammatory stimuli from microbial pathogens, such as endotoxin LPS, are well recognized for their ability to induce pulmonary inflammation; LPS is the major component of the outer membrane of Gram-negative bacteria; LPS can act as endotoxin and bind to its receptor on the cell membrane, initiating a series of innate immune responses⁶.

In animals, LPS challenge induces rapid infiltration of polymorphonuclear leukocyte, leading to the release of inflammatory mediators, cytokines and chemotactic factors⁷. Subsequently, inflammation is induced in alveolar space and the epithelial-endothelial barrier is disrupted, resulting in lung injury⁸.

The complexing of LPS and surfactant may alter the physiologic properties of surfactant *in vitro*⁹. However, little is known about the effect of LPS on SP-B by the intratracheal administration *in vivo*, and the influence of LPS on SP-B in alveolar type II epithelial cells remains poorly defined. Therefore, the aim of this work was to evaluate the effect of LPS on expression and function of SP-B in lung tissue and alveolar type II epithelial cells.

Materials and Methods

Model of LPS-Induced Acute Lung Injury

Six to eight-week-old adult Sprague-Dawley rats (supplied by the laboratory animal center, Institute of Surgery Research, Third Military Medical University, China) were used for these studies, and were anaesthetized with intraperitoneal pentobarbital (50 mg/kg) and orally intubated with a sterile plastic catheter, and challenged with intratracheal instillation of 800 µg of LPS (*E. coli* 0111:B4, Sigma-Aldrich, St. Louis, MO, USA) dissolved in 50 µl of normal saline. Sham-operated animals underwent the same procedure with intratracheal injection of equal saline to serve as controls¹⁰. All animal experiments were performed in accordance with protocols approved by the Committee for the Ethics of Animal Care and Experiments at Third Military Medical University.

Histological Analysis

Rats were humanely killed at 4 h after LPS challenge to collect tissues for analysis. The lung tissues were fixed in 4% paraformaldehyde, embedded in paraffin, and cut into 5 µm thick sections. Sections were stained with hematoxylin and eosin, and images were taken with an Olympus microscope for any alterations in morphology¹¹.

Immunohistochemical Staining

Sections were blocked in a buffer containing 10% normal goat serum, 0.5% bovine serum albumin (BSA) and 0.5% Triton X-100 in phosphate buffered saline (PBS) for 1 h at room temperature. Rinsed sections were incubated overnight at 4°C with primary antibody diluted at different ratios in 1% normal serum, 0.5% BSA and 0.5% Triton X-100 in PBS at 4°C.

After washing, sections were incubated with FITC and/or TRITC conjugated secondary antibodies (1:1000) (Santa Cruz Biotechnology, Santa Cruz, CA, USA) in the dark for 2 hours at room temperature, DAPI (Santa Cruz Biotechnology, Santa Cruz, CA, USA) was applied in order to visualize nuclei of all cells in the studied area of the rat lung. Sections were then washed, dried, mounted, and studied using an upright compound epifluorescent microscope^{12,13}.

RNA Preparation and RT-PCR Amplification

Total RNA was isolated from the lung of the rat using RNeasy Mini kit (Takara, Dalian, China) following the protocol recommended by the

manufacturer. 1 µg total RNA was reverse transcribed using a reverse First-Strand cDNA Synthesis Kit product (Takara, Dalian, China). The primers SP-B-F (5' TTTGAATTCATGCTCCCATCCCTC TGC3') and SP-B-R (5' AAAGGATCCAGTGGAAACATCGGAGGACC AGGCC3') were to amplify the SP-B fragments. PCR was performed in 2.5 µl 10X Reaction Buffer, 2 µl cDNA, 0.5 µl dNTP, 1 µl SP-B-F, 1 µl SP-B-R, 0.2 µl Taq DNA polymerase, 18 µl RNase-Free Water. Amplification was performed for 35 cycles under the following PCR conditions: 30 seconds at 94°C, 30 seconds at 60°C, 30 seconds at 72°C, and 7 minutes at the extension at 72°C using Biometra PCR system. PCR products were then separated electrophoretically on 2% agarose gels and visualized after ethidium bromide staining. The expected product size was 252 bp¹⁴.

Construction of Plasmids

Standard procedures were used for plasmid isolation, restriction endonuclease digestion, ligation and other molecular biology techniques [15]. The SP-B fragments (containing engineered *EcoRI-BamHI* ends) were inserted into the plasmid pUC-T to produce pUC-T-SP-B, and sequenced to check their authenticity. Then, the SP-B fragments were cloned into plasmid pEGFP-N2 to form pEGFP-N2-SP-B, and the resulting constructions were confirmed by DNA sequencing.

Alveolar Type II Epithelial Cell Culture and Transfection

The CCL149 cells were cultured in RP-1640, supplemented with 10% fetal bovine serum (FBS) and 1% penicillin-streptomycin in a humidified 5% CO₂ atmosphere at 37°C. The medium was changed every other day. Cells were trypsinized at 90% confluency with 0.05% trypsin (Thermo Fisher Scientific, Shanghai, China). CCL149 cells were seeded in 24-well dishes (0.5 × 10⁵ cells) in 500 µl of growth medium without antibiotics, a day before transfection. 0.8 µg pEGFP-N2-SP-B recombinant plasmid and PLNCX pEGFP-N2 was diluted in 250 µl into Dulbecco's Modified Eagle Medium (DMEM) without serum. Two microliters of Lipofectamine were diluted in 250 µl DMEM without serum and incubated for 20 min at room temperature. After incubation, the medium with the complexes was removed afterward and fresh full growth medium was added to the cells. After 6 h incubation,

DEME without serum was replaced by DEME with serum, and the different concentration of LPS was simultaneously added to stimulate. The transfected cells were cultured for another 24-48 hours before further analysis by fluorescence microscope¹⁶.

Raman Spectroscopic Analysis of Cell

The alveolar type II epithelial cell CCL149 culture and transfection were as above. After transfection, 0.25% trypsinase were added into CCL149 cell with pEGFP-N2-SP-B for hydrolyzation, then washed twice, rinsed, and immersed in PBS. The treated cells were stimulated by LPS at the final concentration of 50 ng/ml, while the control was not. The treated and control cells were used for the measurement of Raman spectra of single cells, respectively¹⁷.

The system is a confocal device (HORIBA, LabRAM HR Evolution, 533 nm, 20 mW). A laser beam from it was circularized with a pair of anamorphic prisms, spatially filtered, and then introduced in an inverted differential interference contrast (DIC) microscope equipped with the objective to form a single-beam optical trap. The spectral resolution of our confocal micro-Raman system was estimated to be 4 cm^{-1} approximately. The laser power was set at 15 mW and the Raman acquisition time was 15 sec. These conditions were kept constant for all measurements.

Raman spectra of individual cells were obtained through the scan-excitation mode. The background spectra of the solution were acquired with the same scan area without the cell. The spectral process procedure of individual cells includes subtraction of background spectra, intensity calibration, baseline calibration and normalization, and discrimination analysis was carried out using the software Origin 7.5¹⁸.

Results

Histopathological Analysis

The animals were subjected to LPS or sham procedures. Histological assessment of lung sections 4 hours after the administration of LPS with or without treatment was performed. LPS caused marked damage to the lungs, very extensive hemorrhages were seen on surfaces of the collapsed lungs (data not shown). Microscopic evaluation of lung samples revealed severe intra-alveolar and endobronchial hemorrhages. The histological patterns of lung injury due to LPS are shown in Figure 1. Figure 1 A depicts a control lung, in which saline was administered intratracheally, the lung was essentially normal in appearance. In Figure 1 B, LPS-induced lung injury was characterized by interstitial and intra alveolar deposits, prominence of intra-alveolar hemorrhage.

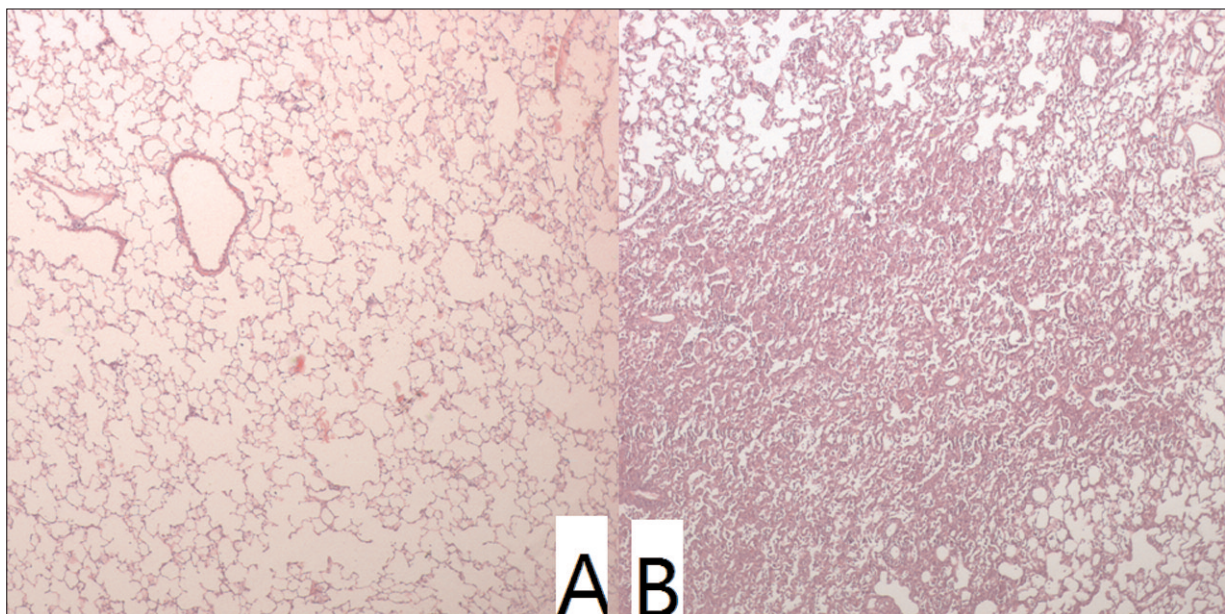


Figure 1. HE staining of lung tissue. **A**, HE staining of normal lung tissue, **B**, HE staining of injury lung tissue. Compared with control, LPS-induced treatment resulted in severe bleeding in lung, defects in the lung alveolar expansion, and intra alveolar deposits.

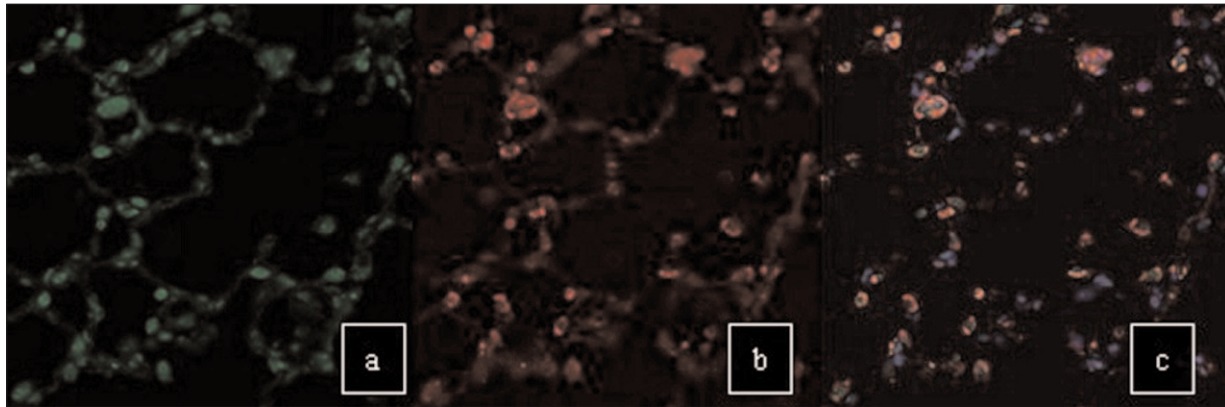


Figure 2. Immunohistochemical analysis of normal lung tissue for surfactant proteins, it shows the localization of SP-B and SP-C in the normal lung, **a**, Location of SP-C, **b**, Location of SP-B, **c**, Location of overlay

Localization of SP-B and SP-C Protein in Rat Lung

We investigated the localization of SP-B and SP-C proteins in normal or LPS-induced injury lung. Nuclei were counterstained with DAPI, SP-B were counterstained with TRITC, and SP-C were counterstained with FITC. SP-B and SP-C proteins showed the same pattern of expression in normal lung. They localized in the alveolar cavity, the fluorescent ring indicated that they dispersed on the whole surface of alveolar space (Figure 2).

But it is different in the LPS-induced injury lung. The fluorescence and expression intensity of SP-B had diminished, the fluorescent ring nearly vanished because of the alveolar collapse. However, conversely to the SP-B proteins expression in the alveolar, the localization and fluorescence intensity of SP-C proteins were not significantly changed. Contrast to SP-B, the LPS-induced influences on SP-C was poor (Figure 3).

Effect of LPS on the Expression of SP-B in Transfected CCL149

The localization of SP-B in alveolar type II epithelial cells and responsiveness to LPS has been investigated. CCL149 cells were transfected with pEGFP-N2 (null) or pEGFP-N2-SP-B plasmid. The pEGFP-N2 and pEGFP-N2-SP-B strongly expressed in CCL149 cells for the observable fluorescence signal.

CCL149 cells with pEGFP-N2 showed the fluorescence signal predominantly in the cytoplasm, CCL149 cells with pEGFP-N2-SP-B showed the fluorescence signal predominantly in the nuclear compartment and on the cell surface with hollow texture, it is meant that the SP-B had the characteristic of exclusive cell surface localization (Figure 4 and Figure 5).

We observed an LPS-induced decrease in the fluorescence intensity of transfected cells stimulated with LPS, and the negative control cells

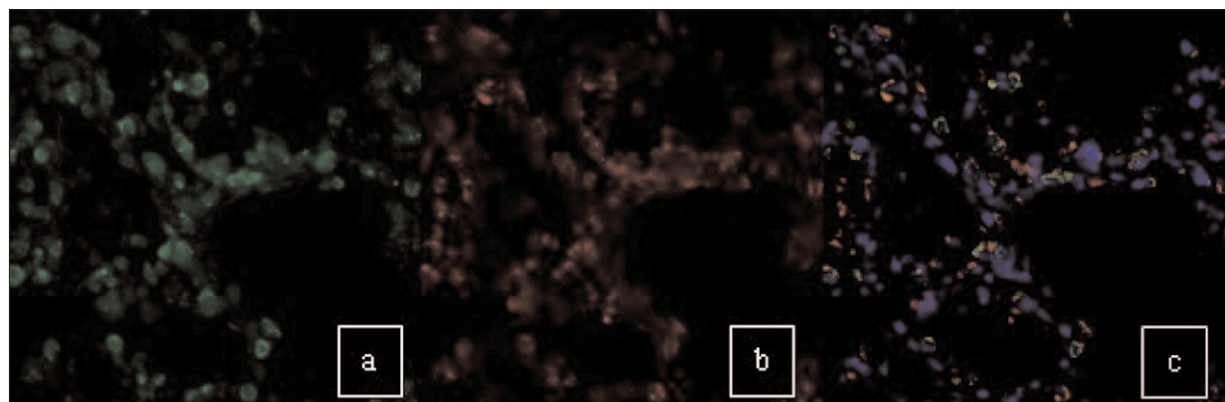


Figure 3. Immunohistochemical analysis of injury lung tissue for surfactant proteins, it shows the localization of SP-B and SP-C in the injury lung, **a**, Location of SP-C, **b**, Location of SP-B, **c**, Location of overlay.

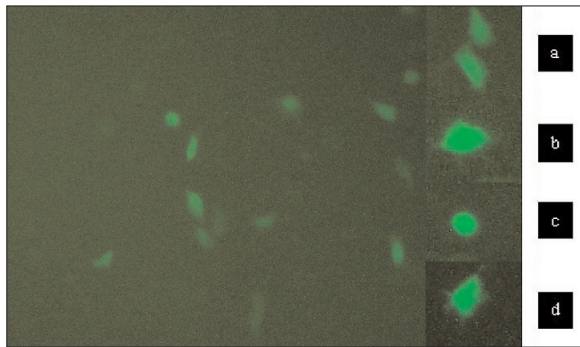


Figure 4. The localization of the pEGFP-N2 in CCL-149 cells, CCL149 cells with pEGFP-N2 showed the fluorescence signal predominantly in the cytoplasm.

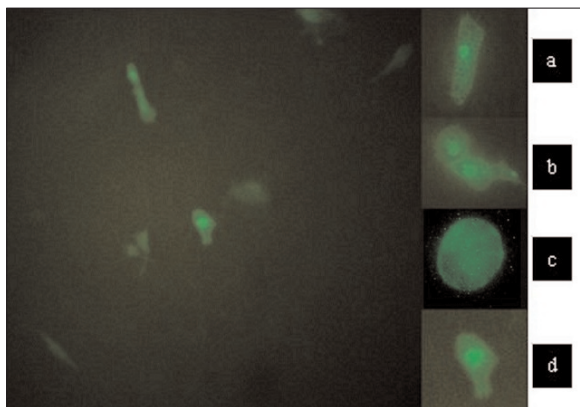


Figure 5. The localization of the pEGFP-N2-SP-B in CCL-149 cells, CCL149 cells with pEGFP-N2-SP-B showed the fluorescence signal predominantly in the nuclear compartment and on the cell surface.

completely lacked fluorescence. For the LPS-stimulated cells, the fluorescence intensity gradually weakened correlating with gradually increased stimulating concentration of LPS (Figure 6).

Analysis of Raman Spectra

The averaged Raman spectra of CCL149 cells with pEGFP-N2-SP-B and CCL149 cells with pEGFP-N2-SP-B treated by LPS are shown in Figures 7 and 8, the spectra of the control and treated groups were averaged over 20 cells that were measured. The position of Raman bands at 1446 cm^{-1} was marked in Figure 7, Raman spectra of untreated CCL149 cells with pEGFP-N2-SP-B and LPS-treated CCL149 cells with pEGFP-N2-SP-B were the curve a and curve b. The band 1446 cm^{-1} corresponds to CH_2 bending vibrations in the proteins and lipids of the cell. After treated by LPS, the CCL149 cells showed lower peak heights in the 1446 cm^{-1} band, which corresponds to the vibrations from proteins and lipids.

The Raman spectra of CCL149 cells in the C-H stretching mode region ($2700\text{-}3000\text{ cm}^{-1}$) was obtained from Figure 8, the position of Raman bands at $2935, 2880\text{ cm}^{-1}$ were marked. The I_{2880}/I_{2935} spectral parameters for CCL149 cells with pEGFP-N2-SP-B is lower than LPS-treated CCL149 cells with pEGFP-N2-SP-B, which were 0.7387 (curve c) and 0.8563 (curve d) respectively.

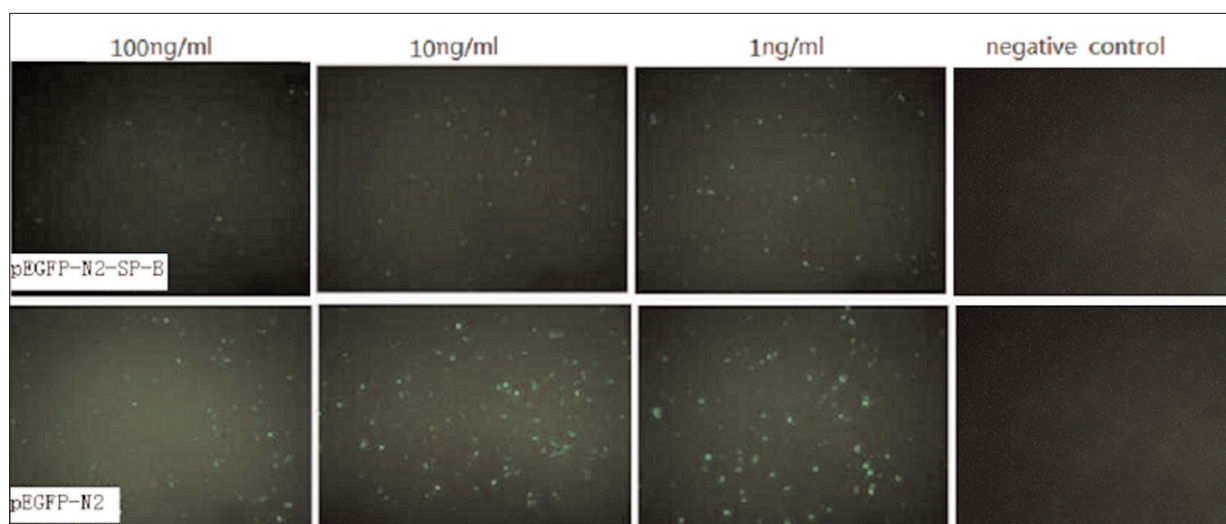


Figure 6. The effect of LPS on the expression of SP-B in transfected CCL149 cells the negative control is CCL149 cell (pEGFP-N2) with no fluorescence, and the fluorescence intensity gradually weakened in CCL149 cell (pEGFP-N2-SP-B) correlating with gradually increased stimulating concentration of LPS.

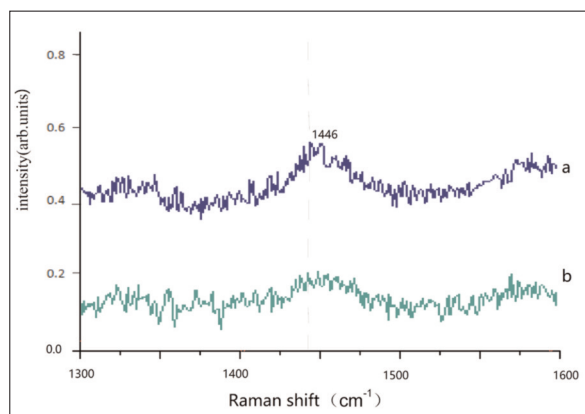


Figure 7. Raman spectra of untreated CCL149 cells with pEGFP-N2-SP-B (curve a) and LPS-treated CCL149 cells with pEGFP-N2-SP-B (curve b). The position of Raman bands at 1446 cm^{-1} were marked.

Discussion

SP-B has a large proportion (52%) of hydrophobic amino acids, and also has cationic characteristics with a net charge of +7 (per monomer) at neutral pH. Its positive charge and highly hydrophobic nature are thought to provide the basis for interactions between SP-B and the negatively charged lipid components of lung surfactant^{19,20}. SP-B is a highly conserved member of the saposin superfamily of proteins and, thus, expected to possess 4 to 5 helices. It is found in the lung as a covalently linked homodimer, with 79 amino acid residues in each monomer. Three intramolecular disulfide bonds are formed by six

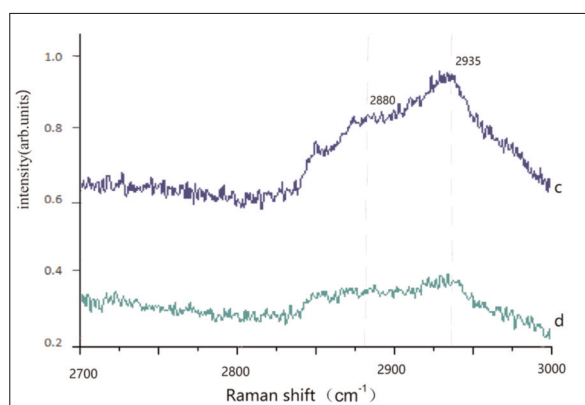


Figure 8. Raman spectra of the C-H stretching mode region ($2700\text{--}3000\text{ cm}^{-1}$), curve c, untreated CCL149 cells with pEGFP-N2-SP-B ($I_{2880}/I_{2935} = 0.7387$), curve d, LPS-treated CCL149 cells with pEGFP-N2-SP-B ($I_{2880}/I_{2935} = 0.8563$). The position of Raman bands at $2935, 2880\text{ cm}^{-1}$ were marked.

cysteines, and a seventh cysteine forms an intermolecular bridge to stabilize the SP-B homodimer structure²¹⁻²³.

In the past years, a number of studies of LPS-induced lung injury focused on the physiology course and mechanism that the lung parenchyma is damaged by the generation and release of proteases and reactive oxygen and nitrogen species, which were produced by activated lung macrophages and transmigrated neutrophils in the interstitial and alveolar compartments²⁴⁻²⁷, even though LPS is known to be an activator of the complement system via the classical and the alternative pathways. However, the direct influences of LPS on alveolar type II epithelial cells and its SP-B had not been shown, which is an impediment to understanding its detailed mechanism²⁸⁻³⁰.

The present results indicated that LPS can directly affect the expression of SP-B, but have a little influence on the similar hydrophobic SP-C, though they are both hydrophobic membrane proteins of alveolar type II epithelial cells. So severe damage to the lung happened after administration of LPS by intratracheal instillation for SP-B reducing, which is the only essential protein component of lung surfactant.

As to normal alveolar type II epithelial cells, the SP-B had the membrane embedded features and localized on the cell surface of CCL149 *in vitro*. It is confirmed that the expression of SP-B was decreased by stimulating the LPS in alveolar type II epithelial cells.

The reduction in the Raman bands observed suggests that the amount of protein and lipid could be lower in the LPS-treated cells. This spectral finding was consistent with the fact that SP-B was reduced in alveolar type II epithelial cells after stimulated by LPS.

The spectral carbon-hydrogen (C-H) intensity ratio, I_{2880}/I_{2935} , where the 2880-cm^{-1} modes refer to the acyl chain methylene (CH_2) asymmetric stretching vibrations, reflects the lateral chain-chain interactions. The 2935-cm^{-1} feature represents a complex spectral interval that contains spectral components interactions involving the chain methylene moieties and the C-H symmetric stretching modes of the chain methyl termini of the lipids.

Disorder/order measures arising from chain-chain interactions are determined from the I_{2880}/I_{2935} intensity parameter. As LPS-treated CCL149 cells with pEGFP-N2-SP-B, the I_{2880}/I_{2935} intensity parameter is higher than it of

untreated CCL149 cells with pEGFP-N2-SP-B. The Raman spectroscopic data suggest that the interaction and stability between SP-B and lipids of LPS-treated CCL149 cells with pEGFP-N2-SP-B perhaps is lower than it of untreated CCL149 cells with pEGFP-N2-SP-B.

The results of this research suggested that we should put more emphasis on the influence on SP-B by LPS in the course of lung injury.

It should be noted that this study has examined only the direct influence of LPS. Of course, it needs to further demonstrate some detail questions, for example, what is the receptor of alveolar type II epithelial cells to LPS, and what is the definite signal way about LPS-induced lung injury in alveolar type II epithelial cells. The microenvironment of the air-water interface is very complex, and the detail influences of LPS on SP-B should be further confirmed.

Conclusions

LPS can directly affect the expression of SP-B *in vivo*, a contrast to SP-B, the LPS-induced influences on SP-C is little. SP-B had the membrane embedded features and localized on the cell surface of CCL149 *in vitro*. The expression of SP-B was decreased by stimulating of LPS in alveolar type II epithelial cells. It is confirmed that the expression of SP-B was decreased by stimulating of LPS in alveolar type II epithelial cells, and it affected the interaction and stability between SP-B and lipids.

Acknowledgements

We acknowledge the support of National Natural Science Foundation of China (Grant No. 81471865), China Postdoctoral Science Foundation (Grant No. 2013M542492) and Chongqing Postdoctoral Science Foundation (Grant No. Xm201348), and the intellectual support of the colleagues in our laboratory.

Conflict of Interest

The Authors declare that there are no conflicts of interest.

References

- 1) POSTLE AD, HEELEY EL, WILTON DC. A comparison of the molecular species compositions of mammalian lung surfactant phospholipids. *Comp Biochem Physiol A Mol Integr Physiol* 2001; 129: 65-73.
- 2) LANG CJ, POSTLE AD, ORGEIG S, POSSMAYER F, BERNHARD W, PANDA AK, JÜRGENS KD, MILSOM WK, NAG K, DANIELS CB. Dipalmitoylphosphatidylcholine is not the major surfactant phospholipid species in all mammals. *Am J Physiol Regul Integr Comp Physiol* 2005; 289: R1426-1439.
- 3) POSSMAYER F. A proposed nomenclature for pulmonary surfactant associated proteins. *Am Rev Respir Dis* 1988; 138: 990-998.
- 4) HAWGOOD S, DERRICK M, POULAIN F. Structure and properties of surfactant protein B. *Biochim Biophys Acta* 1998; 1408: 150-160.
- 5) CLARK JC, WERT SE, BACHURSKI CJ, STAHLMAN MT, STRIPP BR, WEAVER TE, WHITSETT JA. Targeted disruption of the surfactant protein B gene disrupts surfactant homeostasis, causing respiratory failure in newborn mice. *Proc Natl Acad Sci U S A* 1995; 92: 7794-7798.
- 6) MATUTE-BELLO G, WINN RK, MARTIN TR, LILES WC. Sustained lipopolysaccharide-induced lung inflammation in mice is attenuated by functional deficiency of the Fas/Fas ligand system. *Clin Diagn Lab Immunol* 2004; 11: 358-361.
- 7) ROJAS M, WOODS CR, MORA AL, XU J, BRIGHAM KL. Endotoxin-induced lung injury in mice: Structural, functional, and biochemical responses. *Am J Physiol Lung Cell Mol Physiol* 2005; 288: 333-341.
- 8) ALTEMEIER WA, MATUTE-BELLO G, GHARIB SA, GLENNY RW, MARTIN TR, LILES WC. Modulation of lipopolysaccharide-induced gene transcription and promotion of lung injury by mechanical ventilation. *J Immunol* 2005; 175: 3369-3376.
- 9) BROGDEN KA, CUTLIP RC, LEHMKUHL HD. Complexing of bacterial lipopolysaccharide with lung surfactant. *Infect Immun* 1986; 52: 644-649.
- 10) DING N, WANG F, XIAO H, XU L, SHE S. Mechanical ventilation enhances HMGB1 expression in an LPS-induced lung injury model. *PLoS One* 2013; 8: e74633.
- 11) OCHS M. Stereological analysis of acute lung injury. *Eur Respir Rev* 2006; 15: 115-121.
- 12) WANG G, HUANG X, LI Y, GUO K, NING P, ZHANG Y. PPAR-1 Inhibitor, DPQ, Attenuates LPS-Induced Acute Lung Injury through Inhibiting NF-κB-Mediated Inflammatory Response. *PLoS One* 2013; 8: e79579.
- 13) PANG Y, CAI Z, RHODES PG. Disturbance of oligodendrocyte development, hypomyelination and white matter injury in the neonatal rat brain after intracerebral injection of lipopolysaccharide. *Brain Res Dev Brain Res* 2003; 140: 205-214.
- 14) SCHWARTZ DA, CHRIST WJ, KLEEGERGER S R, WOHLFORD-LENANE CL. Inhibition of LPS-induced airway hyperresponsiveness and airway inflammation by LPS antagonists. *Am J Physiol Lung Cell Mol Physiol* 2001; 280: L771-L778.
- 15) MENG F, LOWELL CA. Lipopolysaccharide (LPS)-induced macrophage activation and signal transduction in the absence of Src-family kinases Hck, Fgr, and Lyn. *J Exp Med* 1997; 185: 1661-1670.

- 16) DEMUTH A, CHAKRABORTY T, KROHNE G, GOEBEL W. Mammalian cells transfected with the listeriolysin gene exhibit enhanced proliferation and focus formation. *Infect Immun* 1994; 62: 5102-5111.
- 17) HUANG WE, GRIFFITHS RI, THOMPSON IP, BAILEY MJ, WHITELEY AS. Raman microscopic analysis of single microbial cells. *Anal Chem* 2004; 76: 4452-4458.
- 18) YAO HL, TAO ZH, AI M, PENG LX, WANG GW, HE BJ, LI YQ. Raman spectroscopic analysis of apoptosis of single human gastric cancer cells. *Vib Spectrosc* 2009; 50: 193-197.
- 19) FARVER RS, MILLS FD, ANTHARAM VC, CHEBUKATI JN, FANUCCI GE, LONG JR. Lipid polymorphism induced by surfactant peptide SP-B (1-25). *Biophys J* 2010; 99: 1773-1782.
- 20) LIN S, NA CL, AKINBI HT, APSLEY KS, WHITSETT JA, WEAVER TE. Surfactant protein B (SP-B) *-/-* mice are rescued by restoration of SP-B expression in alveolar type II cells but not clara cells. *J Biol Chem* 1999; 274: 19168-19174.
- 21) WHITSETT JA, NOGEE LM, WEAVER TE, HOROWITZ AD. Human surfactant protein B: structure, function, regulation, and genetic disease. *Physiol Rev* 1995; 75: 749-757.
- 22) SHARIFAHMADIAN M, SARKER M, PALLEBOINA D, WARING AJ, WALTHER FJ, MORROW M R, BOOTH V. Role of the N-Terminal seven residues of surfactant protein B (SP-B). *Plos One* 2013; 8: e72821.
- 23) COLE FS. Surfactant protein B: unambiguously necessary for adult pulmonary function. *Am J Physiol Lung Cell Mol Physiol* 2003; 285: 540-542.
- 24) BAOUKINA S, TIELEMAN DP. Direct simulation of protein-mediated vesicle fusion: lung surfactant protein B. *Biophys J* 2010; 99: 2134-2142.
- 25) REUTERSHAN J, LEY K. Bench-to-bedside review: acute respiratory distress syndrome-how neutrophils migrate into the lung. *Crit Care* 2004; 8: 453-461.
- 26) RAGALLER M, RICHTER T. Acute lung injury and acute respiratory distress syndrome. *J Emerg Trauma Shock* 2010; 3: 43-51.
- 27) ROSSAINT J, NADLER JL, LEY K, ZARBOCK A. Eliminating or blocking 12/15-lipoxygenase reduces neutrophil recruitment in mouse models of acute lung injury. *Crit Care* 2012; 16: 1-15.
- 28) MARSH LM, CAKAROVA L, KWAPISZEWSKA G, VON WULFEN W, HEROLD S, SEEGER W, LOHMEYER J. Surface expression of CD74 by type II alveolar epithelial cells: a potential mechanism for macrophage migration inhibitory factor-induced epithelial repair. *Am J Physiol Lung Cell Physiol* 2009; 296: L442-L452.
- 29) RITTIRSCH D, FLIERL M A, DAY DE, NADEAU BA, MCGUIRE SR, HOESEL LM, IPAKTCHI K, ZETOUNE FS, SARMA JV, LENG L, HUBER-LANG MS, NEFF TA, BUCALA R, WARD PA. Acute lung injury induced by lipopolysaccharide is independent of complement activation. *J Immunol* 2008; 180: 7664-7672.
- 30) STEVEN D, WEINSTEIN D, BLANCO P G, MARTINEZ-CLARK P, URMAN S, ZAMAN M, MORROW JD, ALVAREZ JG. Characterization of LPS-induced lung inflammation in *cftr**-/-* mice and the effect of docosahexaenoic acid. *J Appl Physiol* 2002; 92: 2169-2176.